

# Mutation-specific hemostatic variability in mice expressing common type 2B von Willebrand disease substitutions

Mia Golder,<sup>1</sup> Cynthia M. Pruss,<sup>1</sup> Carol Hegadorn,<sup>1</sup> Jeffrey Mewburn,<sup>2</sup> Kimberly Laverty,<sup>1</sup> Kate Sponagle,<sup>1</sup> and David Lillicrap<sup>1</sup>

<sup>1</sup>Department of Pathology and Molecular Medicine, Richardson Laboratory and <sup>2</sup>Division of Cancer Biology and Genetics, Queen's University Cancer Research Institute, Queen's University, Kingston, ON

**Type 2B von Willebrand disease (2B VWD) results from von Willebrand factor (VWF) A1 mutations that enhance VWF-GPIIb $\alpha$  binding. These “gain of function” mutations lead to an increased affinity of the mutant VWF for platelets and the binding of mutant high-molecular-weight VWF multimers to platelets in vivo, resulting in an increase in clearance of both platelets and VWF. Three common 2B VWD mutations (R1306W, V1316M, and R1341Q) were independently introduced into the mouse *Vwf* cDNA se-**

**quence and the expression vectors delivered to 8- to 10-week-old C57Bl6 *VWF*<sup>-/-</sup> mice, using hydrodynamic injection. The resultant phenotype was examined, and a ferric chloride-induced injury model was used to examine the thrombogenic effect of the 2B VWD variants in mice. Reconstitution of only the plasma component of VWF resulted in the generation of the 2B VWD phenotype in mice. Variable thrombocytopenia was observed in mice expressing 2B VWF, mimicking the severity seen in**

**2B VWD patients: mice expressing the V1316M mutation showed the most severe thrombocytopenia. Ferric chloride-induced injury to cremaster arterioles showed a marked reduction in thrombus development and platelet adhesion in the presence of circulating 2B VWF. These defects were only partially rescued by normal platelet transfusions, thus emphasizing the key role of the abnormal plasma VWF environment in 2B VWD. (*Blood*. 2010;115(23):4862-4869)**

## Introduction

Type 2B von Willebrand disease (2B VWD) is a qualitative variant of VWD, in which there is an increased affinity of the mutant von Willebrand factor (VWF) for platelet glycoprotein IIb/IIIa (GPIIb/IIIa).<sup>1</sup> Inherited in an autosomal-dominant manner, it arises as a result of missense mutations clustered within exon 28 of the VWF gene, the region that encodes the VWF A1 protein domain involved in the binding of VWF to GPIIb/IIIa.<sup>1,2</sup> The gain-of-function phenotype appears to arise through the destabilization of the A1 domain, mimicking the structural changes seen when immobilized VWF is activated through shear stress and allowing the binding of VWF to GPIIb/IIIa in the absence of vascular injury.<sup>3,4</sup> The bleeding phenotype seen in 2B VWD patients probably arises through a multifactorial mechanism: (1) a decrease in plasma high-molecular-weight (HMW) multimers, (2) the occurrence of thrombocytopenia, and (3) the inability of platelets to interact with immobilized VWF at the site of vascular damage.<sup>3</sup> The thrombocytopenia and decrease in HMW multimers arise as a result of increased clearance of both platelets and VWF.<sup>3</sup> In addition, 2B VWF is more susceptible to ADAMTS13-mediated cleavage.<sup>5</sup>

The VWF mutation database lists more than 50 reports of 24 different mutations leading to 2B VWD.<sup>6</sup> Of these, the mutations R1306W, V1316M, and R1341Q are the most common, having been reported 10, 9, and 7 times, respectively.<sup>6</sup> The recent study of Federici et al<sup>7</sup> of a cohort of 67 2B VWD patients showed a heterogeneous clinical presentation, dependent on the VWF A1 domain mutation. Of the 11 mutations present in this cohort, the V1316M mutation resulted in the most significant thrombocytopenia, the highest bleeding scores, and the longest bleeding times. The phenotype associated with the R1306W and R1341Q mutations was less severe than that seen with V1316M but significantly more severe than the phenotype seen with P1266Q/L and R1308L. Both R1306W and R1341Q showed complete loss of HMW

multimers, whereas V1316M showed the additional loss of intermediate MW multimers. In contrast, the P1266Q/L and R1308L mutations showed normal plasma multimer patterns.<sup>7</sup>

Although 2B VWD causes a bleeding phenotype, the presence of circulating platelet aggregates and the activation of circulating platelets by the hyperactive 2B VWF may contribute to an enhanced tendency for arterial thrombotic events. However, both the rarity of 2B VWD and its presence in the context of heterogeneous human genetic backgrounds suggest that studies in inbred mouse models might provide useful answers to these questions. Currently, there is no transgenic mouse model of 2B VWD. There is a VWF knockout (*VWF*<sup>-/-</sup>) mouse model<sup>8</sup> that has been used to create transient models of plasma-based VWD variants, through the introduction of mutant VWF plasmids via hydrodynamic tail vein injection.<sup>9</sup>

Given the clinical variability of 2B VWD, we created mouse models of 2B VWD to examine the 3 most common 2B VWD mutations found in humans: R1306W, V1316M, and R1341Q. Our goals were to determine whether the variable clinical phenotype documented in 2B VWD patients could be reproduced in the inbred mouse model and to evaluate the thrombogenic potential of the murine 2B VWD variants. Together, these studies provide novel insights into the unique gain-of-function phenotype observed in 2B VWD.

## Methods

### Animals

C57Bl/6 wild-type and C57Bl/6 VWF knockout<sup>8</sup> mice, 8 to 10 weeks of age, were used in all experiments. All mouse experiments were reviewed and approved by the Queen's University Animal Care Committee.

Submitted November 18, 2009; accepted March 16, 2010. Prepublished online as *Blood* First Edition paper, April 6, 2010; DOI 10.1182/blood-2009-11-253120.

The publication costs of this article were defrayed in part by page charge

payment. Therefore, and solely to indicate this fact, this article is hereby marked “advertisement” in accordance with 18 USC section 1734.

© 2010 by The American Society of Hematology

## Construction of plasmids

The full-length murine VWF cDNA (*mVwf*, kindly provided by Dr Peter Lenting) was inserted into the pCIneo plasmid (Promega).<sup>10</sup> Mutagenesis was performed using the Quikchange Site-Directed Mutagenesis Kit (Stratagene) to introduce the R1306W, V1316M, and R1341Q mutations. Long-term in vivo transgene expression was obtained through the insertion of the wild-type or mutant mVWF into the pSC11 plasmid<sup>11</sup> containing the synthetic, liver-specific enhanced transthyretin (ET) promoter (kindly provided by Dr Luigi Naldini).<sup>12</sup>

## Recombinant VWF protein production

Calcium phosphate transient transfection was performed using HEK293T cells, as previously described.<sup>13</sup> Recombinant mouse VWF (mVWF) was secreted into serum-free OptiMEM containing 100 U/mL penicillin, 100 µg/mL streptomycin, and 1 times insulin/selenium/transferrin G (Invitrogen), and the medium harvested 72 hours after transfection. mVWF was concentrated using Amicon Centricon-Plus 70 centrifugal filter units (Millipore).

## VWF levels and structure

Plasma VWF was quantified through an enzyme-linked immunosorbent assay (ELISA), using a polyclonal rabbit anti-human VWF antibody and a horseradish peroxidase-conjugated polyclonal rabbit anti-human VWF antibody (Dako North America).<sup>8</sup> Pooled plasma from 30 C57Bl/6 wild-type mice was used as a reference.

The multimeric structure of VWF was analyzed using a 1.4% separating sodium dodecyl sulfate agarose gel; polyclonal horseradish peroxidase-conjugated anti-human VWF antibody (Dako North America) was used to visualize the multimers through chemoluminescent-based imaging.<sup>14</sup> Lanes were analyzed for migration distance using alphaeasefc, Version 3.1.2 (Alpha Innotech), and low-molecular-weight (bands 1-5), intermediate-molecular-weight (bands 6-10), and HMW (> 10 bands) multimers were counted and the loss of multimer bands assessed.

## ADAMTS13 digestion

Recombinant murine ADAMTS13 (rADAMTS13, kindly provided by Dr Friedrich Scheiflinger) was serially diluted in 5mM Tris (tris(hydroxymethyl)aminomethane), pH 8.0, and activated with 10mM BaCl<sub>2</sub> for 5 minutes at 37°C. A total of 25 µL of rADAMTS13 was added to 25 µL of rVWF (1 U/mL in 1.5M urea, 5mM Tris) and incubated for 24 hours at 37°C. The reactions were stopped through the addition of ethylenediaminetetraacetic acid at a final concentration of 50mM.<sup>15</sup> Samples were frozen at -80°C until multimer analysis. Analysis of the relative multimer migration was performed as previously described.<sup>13</sup>

## Platelet-binding assay

Platelet binding was performed as described previously, with modifications.<sup>2</sup> A total of 25 mU/mL mVWF was incubated with and without formalin-fixed mouse platelets (1 × 10<sup>9</sup> platelets/L in 100mM Tris, pH 7.5, 150mM NaCl, and 3% bovine serum albumin). Freshly prepared botrocetin (Pentapharm) was added, and reactions were incubated at room temperature for 150 minutes. The reactions were centrifuged for 5 minutes at 18 000g, and the supernatant was used in a VWF ELISA to determine the amount of bound VWF.

## Hydrodynamic injection

Plasmid DNA (100 µg) was diluted in a volume of lactated Ringer solution equal to 10% of mouse body weight and injected into the tail vein of C57Bl/6 VWF<sup>-/-</sup> mice in 6 seconds.<sup>9</sup> A 27-gauge needle and a 3-mL syringe were used for the injections.

## Blood collection

Mice were anesthetized using isoflurane/oxygen. Blood samples were obtained via the retro-orbital plexus using uncoated microhematocrit

capillary tubes (Fisher Scientific) and mixed with one-tenth volume 3.2% sodium citrate. Samples were centrifuged at 11 000g at room temperature for 5 minutes, and the resulting platelet-poor plasma was stored at -80°C until tested. Blood samples used to make blood smears were obtained in the same manner, with ethylenediaminetetraacetic acid as an anticoagulant.

## Ferric chloride-induced thrombosis

Intravital microscopy was performed using a trinocular Wild-Leitz ELR-intravital microscope (Leica Microsystems Canada) fitted with both transmitted (50 W halogen) and fluorescence (50 W mercury incidence) light accessories. Images of thrombosis formation were captured by a Hamamatsu ORCA ER video camera with fluorescent light. Analysis of the formed thrombi and the accumulated fluorescence intensity was performed using Image ProPlus, Version 6.0 (Media Cybernetics). Rhodamine 6G (40 ng; Sigma-Aldrich) was injected to fluorescently label platelets in vivo and to facilitate visualization of the formation of the in situ thrombus.

Ferric chloride injury was induced as described previously,<sup>16,17</sup> with slight modifications. Male mice were anesthetized with an intraperitoneal injection of ketamine/xylazine/atropine. The jugular vein was cannulated for injection of rhodamine 6G and the cremaster exteriorized. Throughout the experiment, the muscle was superfused with 37°C saline solution. Arterioles ranging in size from 50 to 75 µm were chosen, and injury was induced through the application of 10% ferric chloride-soaked filter paper (1 × 1 mm) for 3 minutes. After injury, the muscle was flushed with preheated saline and the injured area in a single arteriole observed for 40 minutes. The time to vessel occlusion with thrombus and accumulated fluorescence intensity from images captured at 5-minute intervals were examined.

Washed platelets were obtained from normal C57Bl/6 mice. VWF<sup>-/-</sup> and VWF<sup>-/-</sup> mice expressing V1316M VWF were infused with 5 × 10<sup>7</sup> normal platelets, 5 minutes before ferric chloride induced vascular damage. Intravital microscopy was performed as described.

## Statistical analysis

Data are presented as mean values plus or minus SEM. Statistical analyses were performed using the Student unpaired *t* test, one-way analysis of variance (ANOVA), or 2-way ANOVA. Occlusion times exceeding 40 minutes were recorded as 40 minutes.

## Results

### Platelet-binding assay

The platelet-binding ability of mVWF was examined (Figure 1) using formalin-fixed, washed mouse platelets, mVWF expressing the 2B VWD mutations of interest, and botrocetin. mVWF expressing the V1316M mutation was able to spontaneously bind platelets in the absence of botrocetin (36.6% ± 8.1% bound VWF),

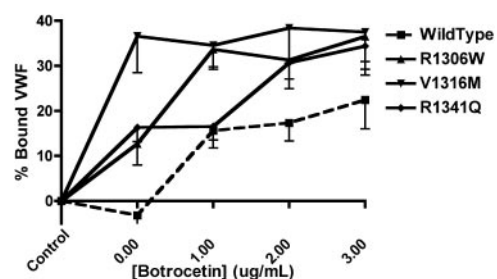


**Figure 1. VWF-platelet binding assay to examine the enhanced binding of recombinant mouse type 2B VWF variants.** Recombinant mVWF was incubated with formalin-fixed mouse platelets in the presence or absence of botrocetin. The amount of bound VWF is expressed as a percentage of a control incubation that was composed of mVWF in the absence of platelets and botrocetin. Data are mean ± SEM of 6 experiments.

whereas mVWF expressing the R1306W and R1341Q mutations showed a lesser degree of spontaneous platelet binding ( $12.7\% \pm 4.7\%$  and  $16.3\% \pm 3.1\%$  bound VWF, respectively). With the highest concentration of botrocetin ( $3 \mu\text{g/mL}$ ), all 3 of the murine 2B VWD mutations showed significantly more platelet binding than the wild-type mVWF ( $P < .05$ , 1-way ANOVA).

### ADAMTS13 cleavage

In the absence of recombinant mADAMTS13, recombinant mVWF showed the full spectrum of multimers. A total of 1 U/mL mVWF was incubated with a range of concentrations of recombinant mADAMTS13 for 24 hours at  $37^\circ\text{C}$ , and the concentration of mADAMTS13 required to cause loss of 50% of multimer height was determined. R1306W, V1316M, and wild-type mVWF were examined. Wild-type mVWF showed 50% loss of multimers with 0.324 U/mL mADAMTS13 (Figure 2). mVWF expressing the R1306W mutation required 36.5% the amount of ADAMTS13 compared with wild-type ( $P < .001$ ,  $t$  test), with 50% loss of multimer height with 0.118 U/mL ADAMTS13. Similarly, mVWF expressing the V1316M mutation also required a reduced concentration of mADAMTS13 to show 50% loss of multimers ( $0.097 \text{ U/mL}$ ;  $P < .001$ ,  $t$  test, compared with WT mVWF). Thus, both the mVWF 2B VWD mutants examined in this study showed an enhanced susceptibility for ADAMTS13-mediated cleavage, a phenomenon that recapitulates findings with human 2B VWD mutants.<sup>5</sup>

### VWF transgene expression

VWF:Ag was monitored in the mice injected with the mVWF expression plasmids. Peak VWF levels were seen at day 3 (Figure 3A). When the VWF:Ag dropped below 1.5 U/mL, intravital microscopy was performed on the male mice. The mice expressing the V1316M mutation had mean VWF:Ag levels that were the first to drop below 1.5 U/mL, with a mean VWF:Ag of 1.29 plus or minus 0.65 U/mL on day 14 (Figure 3B). At the same time point, mice expressing wild-type VWF had a mean VWF:Ag of 7.83 plus or minus 3.10 U/mL, the R1306W mutation a VWF:Ag of 2.30 plus or minus 0.66 U/mL, and the R1341Q mutation a VWF:Ag of 6.47 plus or minus 1.56 U/mL. By day 21, the mice expressing wild-type VWF had a mean VWF:Ag of 4.02 plus or minus 1.21 U/mL, whereas the mean VWF:Ag levels in the type 2B VWD transgenic mice were significantly lower ( $P < .05$ , 1-way ANOVA). R1306W had a mean VWF:Ag of 1.47 plus or minus 0.56 U/mL, V1316M had a mean VWF:Ag of 0.97 plus or minus 0.40 U/mL,

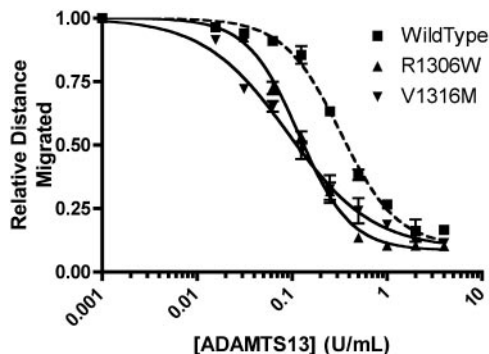


**Figure 2. Analysis of recombinant mouse ADAMTS13 digestion of recombinant mouse VWF.** A total of 1 U/mL mVWF was digested with various concentrations of recombinant mADAMTS13 for 24 hours at  $37^\circ\text{C}$ . Distances were graphed using a 4-parameter curve, and the concentration of mADAMTS13 required to cause loss of 50% of multimer height was determined. Data are mean  $\pm$  SEM of 2 experiments.

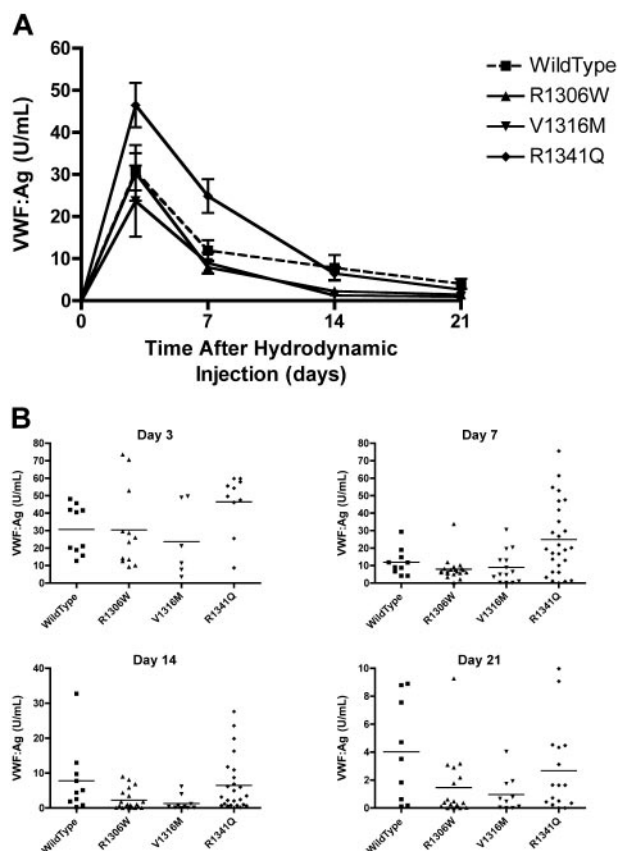


**Figure 3. Plasma VWF levels after hydrodynamic injections.** Plasma samples were obtained after hydrodynamic injections and VWF:Ag was determined using a VWF:Ag ELISA. (A) Time course of plasma VWF:Ag. Data are mean  $\pm$  SEM. (B) VWF:Ag at each time point. Each symbol represents one mouse.

and R1341Q had a mean VWF:Ag of 2.67 plus or minus 0.78 U/mL (Figure 3B).

### Platelet count and blood smear morphology

The mice expressing the type 2B VWD mutations showed thrombocytopenia that fluctuated over time (Figure 4A-B). At day 7, the mice expressing R1306W mutation were the most thrombocytopenic with a mean platelet count of 150 plus or minus  $20 \times 10^9/\text{L}$ . Mice expressing wild-type VWF had a mean platelet count of 370 plus or minus  $39 \times 10^9/\text{L}$ , whereas the other type 2B variants, V1316M and R1341Q, were both associated with significantly lower mean platelet counts of 157 plus or minus  $13 \times 10^9/\text{L}$  and 194 plus or minus  $24 \times 10^9/\text{L}$ , respectively ( $P < .001$ , one-way ANOVA). At day 21, the mice expressing the V1316M mutation had the lowest platelet count ( $180 \pm 36 \times 10^9/\text{L}$ ;  $P < .01$ ,  $t$  test), whereas the other type 2B VWD mutations were also associated with lower mean platelet counts (Figure 4B): R1306W 201 plus or minus  $37 \times 10^9/\text{L}$  ( $P < .05$ ,  $t$  test) and R1341Q 303 plus or minus  $47 \times 10^9/\text{L}$  ( $P = .22$ ,  $t$  test).

Blood smears were made using blood samples taken at day 7 to evaluate the presence of platelet aggregates and enlarged platelets. As seen in Figure 4C, blood smears made from mice expressing the V1316M mutation showed many platelet aggregates containing some large platelets. Platelet aggregates were not seen in blood smears from VWF<sup>-/-</sup> mice expressing wild-type VWF. Blood smears made from mice expressing the R1306W and R1341Q mutations also showed small platelet aggregates; and in the

aggregates associated with the R1306W mutant protein, some large platelets were observed.

**VWF multimer profile**

To determine whether mice expressing the 2B VWD variants showed loss of HMW multimers, plasma samples from multiple days were examined for the number of multimer bands, as shown in Figure 5A. There was some loss of HMW multimers in samples from mice expressing wild-type VWF, but the mice expressing the 2B VWD variants showed a greater extent of HMW multimer loss. By day 7, mice expressing the 2B VWD variants showed complete

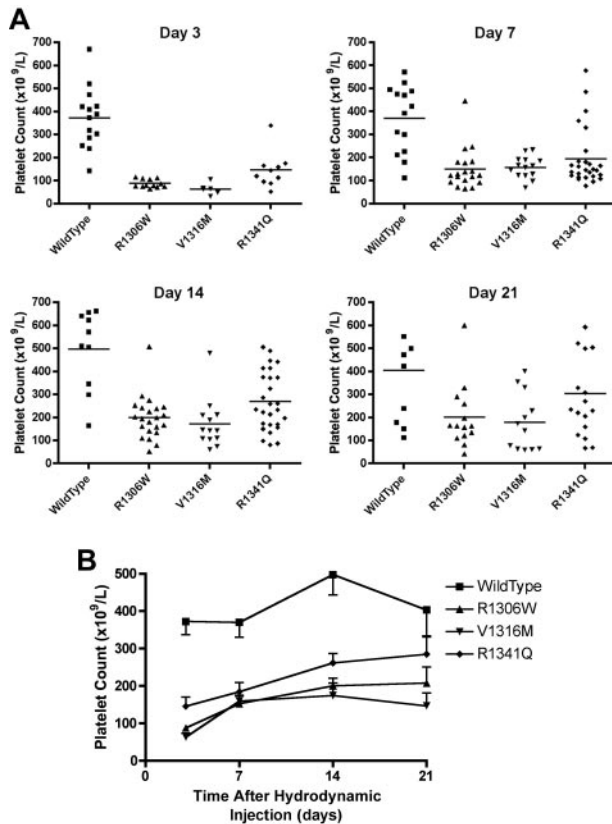


**Figure 4. Platelet count and blood smear morphology.** After hydrodynamic injection, mice were regularly sampled and complete blood counts were performed. Seven days after hydrodynamic injections, samples were also obtained for blood smear examination. (A) Platelet count at each time point. Each symbol represents one mouse. (B) Time course of platelet count after hydrodynamic injection. Data are mean  $\pm$  SEM. (C) Typical blood smear from a mouse expressing the V1316M mutation. A large platelet aggregate is circled within which there are a number of enlarged platelets. Blood smears were observed using an Olympus BX60 transmitted microscope fitted with a UPlanApo 40 $\times$  oil objective. Microscopic images were captured using a Nikon DXM1200 camera and Nikon Act-1 software. Photoshop (Adobe) was used to manipulate the blood smear images.

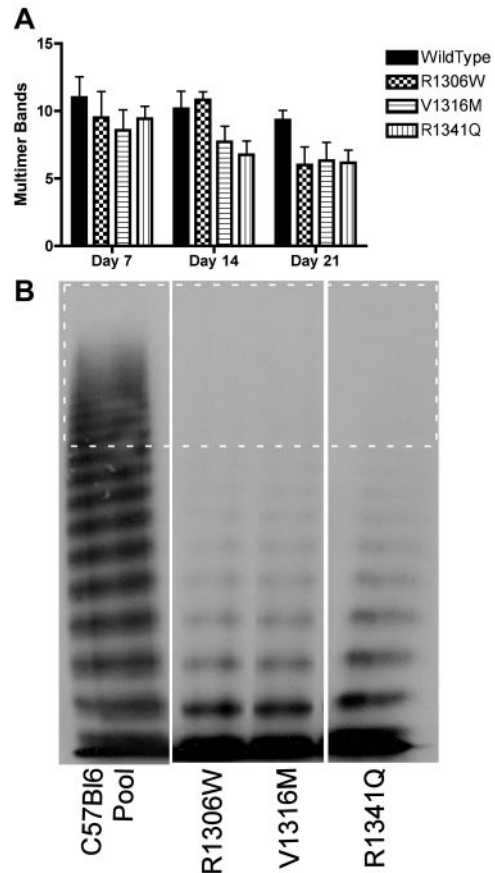


**Figure 5. VWF multimer formation after hydrodynamic injection.** Plasma samples were obtained at different time points after hydrodynamic injection and were analyzed for VWF multimer structure using 1.4% sodium dodecyl sulfate separating agarose gel electrophoresis. (A) Time course of the decreasing number of multimer bands. Data are mean  $\pm$  SEM. (B) Representative multimers of plasma samples obtained at day 14. The dotted rectangle surrounds the HMW multimer bands (> 10 bands).

loss of HMW multimers; and by day 14, mice expressing the V1316M and R1341Q mutations also showed loss of intermediate MW multimers (Figure 5A-B).

**Intravital microscopy**

Intravital microscopy was performed on male mice with VWF:Ag levels less than 1.5 U/mL. After cremaster arteriolar damage with 10% ferric chloride for 3 minutes, the vessel was observed for 40 minutes. During the 40-minute observation period, occlusive thrombi were not documented in any of the mice expressing V1316M. One mouse expressing R1306W and one mouse expressing R1341Q showed occlusive clots (Figure 6A). In both cases, the clots that formed were highly unstable and embolized after 3 minutes. The rest of the mice expressing these mutations did not show any occlusive clots. None of the VWF<sup>-/-</sup> mice showed any occlusive clots (Figure 6A). The VWF<sup>-/-</sup> mice expressing wild-type VWF had a mean time to vessel occlusion of 29.9 plus or minus 2.1 minutes ( $P < .001$ , 1-way ANOVA).

At 5-minute intervals after ferric chloride-induced vessel injury, accumulated fluorescence intensity was measured as a surrogate for platelet accumulation (Figure 6B). At each time point examined, the mice expressing the 2B VWF variants showed significantly less platelet accumulation than both the VWF<sup>-/-</sup> mice and the VWF<sup>-/-</sup> mice expressing wild-type VWF ( $P < .001$ ; 2-way ANOVA). Examination of the area under the accumulated

fluorescence curve (Figure 6C) showed that the mice expressing V1316M had the least platelet accumulation, followed by the mice expressing R1306W and R1341Q. In contrast, some platelet accumulation was seen with the VWF<sup>-/-</sup> mice, although significantly more platelets adhered to the site of injury in the VWF<sup>-/-</sup> mice expressing wild-type VWF ( $P < .05$ , 1-way ANOVA).

We finally evaluated the influence of platelets on the thrombogenic and platelet adhesive processes in the context of different plasma VWF environments. Before ferric chloride induced vascular damage, VWF<sup>-/-</sup> mice and mice expressing the V1316M mutation, with VWF:Ag levels below 1.5 U/mL, were transfused with platelets isolated from normal C57Bl/6 mice. During the 40-minute observation period, there was a significant decrease in the mean time to occlusion in both the transfused VWF<sup>-/-</sup> mice (mean time to occlusion,  $25.0 \pm 3.1$  minutes) and the V1316M mice (mean time to occlusion,  $34.1 \pm 2.5$  minutes) compared with those that had not received platelet transfusions ( $P < .001$ , 1-way ANOVA).

Fluorescence intensity was again used as a surrogate measure for platelet accumulation in these experiments. Examination of the area under the accumulated fluorescence curve (Figure 7B) showed that the mice expressing V1316M that had received a platelet

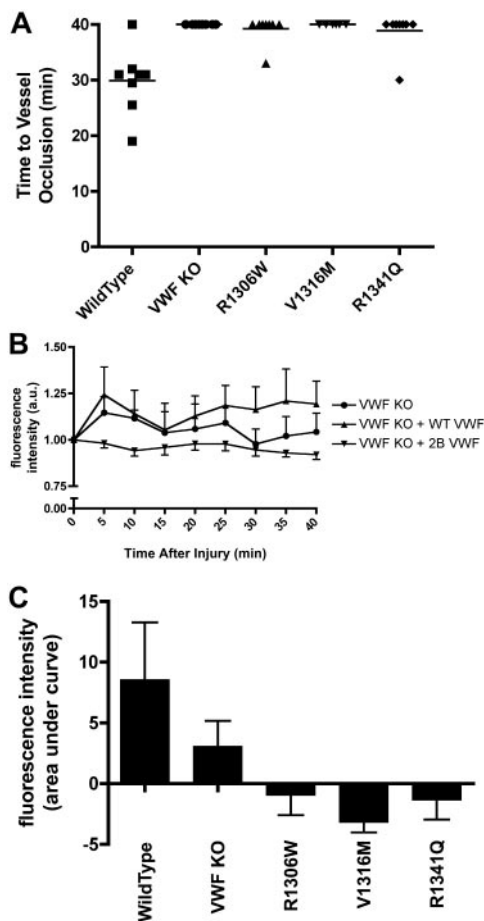


**Figure 6. Thrombus formation and platelet accumulation at sites of endothelial damage in hydrodynamically injected mice.** A total of 10% ferric chloride was used to injure cremaster muscle arterioles (50–75  $\mu$ m in diameter). The vessels were observed for 40 minutes, and fluorescence intensity was measured every 5 minutes as a measure of platelet accumulation. Hydrodynamically injected mice were examined when plasma VWF:Ag dropped below 1.5 U/mL. (A) Time to vessel occlusion. Each symbol represents one mouse. (B) Fluorescence intensity over time. Data are mean  $\pm$  SEM. Type 2B data are the mean  $\pm$  SEM of the 3 mutations. (C) Total fluorescence accumulation, represented as the area under curve of fluorescence intensity.

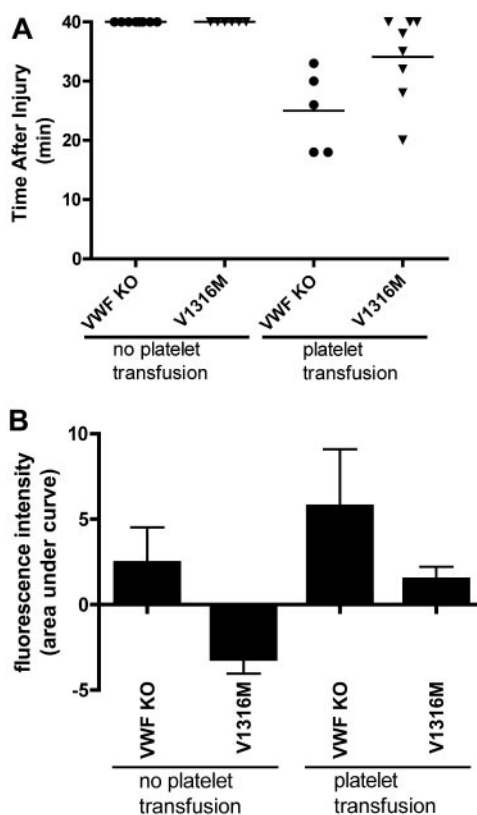


**Figure 7. Thrombus formation and platelet accumulation at sites of endothelial damage in hydrodynamically injected mice after platelet transfusion.** A total of 10% ferric chloride was used to injure cremaster muscle arterioles after transfusion with C57Bl/6 normal platelets. The vessels were observed for 40 minutes; fluorescence intensity was assessed every 5 minutes as a surrogate measure for platelet accumulation. (A) Time to vessel occlusion. Each symbol represents one mouse. (B) Total fluorescence accumulation, represented as the area under the curve of fluorescence intensity.

transfusion experienced significantly more platelet accumulation than those that had not received a platelet transfusion ( $P < .05$ , Bonferroni post-test). After platelet transfusion, the platelet accumulation in the V1316M expressing mice was similar to that seen in the VWF<sup>-/-</sup> mice.

## Discussion

The VWF A1 domain mutations evaluated in this study, R1306W, V1316M, and R1341Q, were chosen for 3 reasons. First, of the 2B VWD causative mutations listed in the VWF mutation database, these 3 mutations account for almost 50% of reports.<sup>6</sup> Second, these mutations have been shown to result in variably severe phenotypes.<sup>7</sup> Finally, the wild-type residues at each of these mutation sites are conserved between the human and mouse Vwf cDNA sequence, implying functional significance of these amino acids. Thus, this study attempted to reproduce the variable clinical phenotype reported in 2B VWD patients in a mouse model in which the plasma VWF compartment was rescued with transgenic mutant VWF. The second aim of the study was to use this mouse model to evaluate the thrombogenic potential of the murine 2B VWD variants.

Type 2B VWD is characterized by the enhanced binding affinity of the mutant VWF to the platelet receptor GPIIb/IIIa, an enhancement that varies in severity dependent on the causative mutation.<sup>1,7</sup> In

this study, the platelet-binding ability of the recombinant mVWF was evaluated in the presence of botrocetin and shown to be mutation-dependent. Botrocetin was selected as a modulator of the VWF-GPIb $\alpha$  interaction, rather than the more commonly used reagent ristocetin. The ability of ristocetin to modulate the interaction of mouse platelets and mVWF has been questioned, probably because of amino acid differences at VWF residues thought to be critical for ristocetin binding.<sup>18,19</sup> Botrocetin modulates VWF-GPIb $\alpha$  through a different mode of action; thus, species specificity is not an issue.<sup>20</sup> At low concentrations of botrocetin, there was variability in the degree of VWF-platelet binding, depending on the mutation examined. At the higher concentrations of botrocetin examined, all 3 mutations showed significantly more VWF-platelet binding than wild-type mVWF. Similar examinations of recombinant human VWF show intermutation similarities in spontaneous and ristocetin-induced platelet-VWF binding.<sup>2</sup>

The 2B VWD patients show loss of plasma VWF HMW multimers, and recombinant human VWF expressing 2B VWD mutations shows increased proteolytic cleavage by recombinant ADAMTS13.<sup>5</sup> Similarly, in our examination of the mVWF 2B mutants R1306W and V1316M, an increased sensitivity to recombinant mADAMTS13 proteolysis was seen. Thus, *in vitro*, mVWF expressing 2B VWD mutations show both increased platelet binding and ADAMTS13 proteolysis, confirming the proposal of Rayes et al that the loss of plasma HMW multimers seen in 2B VWD probably arises through a combination of enhanced platelet binding of mutant HMW multimers and increased proteolysis of the 2B VWF by ADAMTS13.<sup>5</sup>

The variable phenotype seen in 2B VWD patients is dependent on the specific causative mutation. In addition, the variable "outbred" human genetic background, as well as environmental factors, such as stress and pregnancy, can exacerbate the 2B VWD phenotypic spectrum.<sup>21</sup> The development of genetically inbred mouse models of 2B VWD allows for the evaluation of the phenotypic variability of the specific VWF mutations in the absence of these complicating factors. The mice used in this study, C57Bl/6 VWF<sup>-/-</sup> mice, are a strain of highly inbred mice; thus, genetic variability is no longer a factor in the phenotypic differences seen with the expression of the 2B VWD variants in the mouse. Furthermore, the *Vwf* cDNA sequence, which itself is highly polymorphic in humans, was consistent in all of the studies reported here.

Hydrodynamic injection of our expression plasmids results in long-term transient expression of mVWF.<sup>9</sup> The use of the synthetic, liver-specific ET promoter,<sup>12</sup> in combination with the bolus tail vein injection, results in mVWF expression from hepatocytes into the plasma.<sup>9</sup> Importantly, there is no VWF expression in platelets (megakaryocytes), endothelial cells, or the subendothelium with this method of gene delivery.<sup>22</sup> Strategies to target VWF expression to these other compartments will require more complex, time-consuming, and costly technologies.

A dramatic increase in plasma VWF levels, which peaked at day 3, was seen after hydrodynamic injection of the wild-type and 2B variant VWF expression plasmids. Depending on the expression plasmid injected, the VWF:Ag levels dropped to physiologic levels of less than 1.5 U/mL between days 21 and 35 after injection. Mice expressing the V1316M mutation experienced the quickest reduction in VWF:Ag levels, followed by mice expressing R1306W and mice expressing R1341Q, respectively. In 2B VWD patients, similar differences in VWF:Ag are seen: patients with the V1316M mutation have the lowest mean VWF:Ag levels, followed by patients with the R1306W mutation.<sup>7</sup>

Of the mutations examined, 2B VWD patients with the V1316M mutation show the most severe thrombocytopenia, followed by R1306W, then R1341Q.<sup>7</sup> In mice expressing the 2B VWD variants, this thrombocytopenic trend was reproduced, with the V1316M mutation resulting in the lowest platelet counts. Individual 2B VWD patients often show variable thrombocytopenia, with exacerbations occurring at the time of physiologic stress when mutant protein levels are increased. Mice expressing the 2B VWD variants also showed temporal variability in platelet counts. Between each sampling time point, there was considerable variability in platelet counts in individual mice. Interestingly, the variable thrombocytopenia occurred with a transgene promoter that probably does not show the acute-phase responsiveness of the native VWF promoter.

The 2B VWD patients with the R1306W and R1341Q mutations typically have blood smears that show the presence of enlarged platelets but the absence of platelet aggregates, whereas those with the V1316M mutation show platelet aggregates composed of many large platelets.<sup>7</sup> Mice expressing the V1316M mutation had blood smears that recapitulated those seen in patients with this mutation. Similarly, mice expressing the R1306W and R1341Q mutations showed morphologic changes that mimicked the human 2B VWD mutations. As proposed by Nurden et al, in type 2B VWD, there may be enhanced binding of HMW VWF multimers to developing proplatelets that interferes with the normal maturation of platelets, accelerating platelet release and resulting in macrothrombocytopenia.<sup>23,24</sup> The shorter life span of mouse platelets may exaggerate this phenomenon.<sup>23,25</sup> Most noteworthy, the thrombocytopenia and blood smear platelet abnormalities seen in the 2B mice have developed in the presence of mutant VWF expressed only in the plasma compartment, suggesting that expression of the mutant protein in platelets is not required for these phenomena.

Interestingly, the very recent description of the V1316M mutation in patients with the Montreal platelet syndrome<sup>26</sup> has shown that the original families described with this inherited macrothrombocytopenic trait are indeed 2B VWD patients.<sup>27</sup> The phenotype of Montreal platelet syndrome was reproduced in the mice expressing the V1316M mutation, with the presence of both macrothrombocytopenia and platelet clumping on peripheral blood smears.

Despite the inbred background of the mice used in these experiments and the monomorphic *Vwf* cDNA sequence (apart from the 2B VWD mutations), there was variability in the observed phenotype within the 2B VWD variants. In the absence of any obvious physiologic stressors, expression of the 2B VWD variants resulted in significant intermouse and intramouse variability in the observed VWF:Ag levels and platelet counts. These findings suggest that relatively subtle environmental variances can influence the phenotypic spectrum and severity in 2B VWD.

HMW VWF multimers are seen after hydrodynamic injection of mVWF expression plasmids; and in mice expressing the 2B VWF mutants, there is a significant loss of these multimers. Further examination of the VWF multimer profile of mice expressing hydrodynamically delivered VWF shows a lack of the multimer triplets normally seen with endogenous plasma VWF. During endogenous synthesis of VWF in endothelial cells and megakaryocytes, considerable post-translational modifications occurs, with the addition of 12 N-linked and 10 O-linked glycosylation sites to mature monomers.<sup>28</sup> In this study, VWF was expressed from the liver and probably undergoes different patterns of glycan modification to that encountered in the native cells of synthesis. This differential processing probably affects the molecular weight of the

multimer bands and alters the VWF multimer profile. Furthermore, given the influence of glycosylation on ADAMTS13-mediated cleavage of VWF, the expression of transgenic VWF from the liver may also affect its processing by ADAMTS13.<sup>28</sup>

Ferric chloride–induced cremaster arteriolar injury was used to evaluate the thrombogenic potential of murine 2B VWD variants. The effect of vascular damage was examined in male mice with VWF:Ag levels less than 1.5 U/mL. Initial studies with mice hydrodynamically injected with wild-type pSC11-ET-mVWF showed that supraphysiologic levels of circulating VWF in VWF<sup>-/-</sup> mice failed to result in occlusive thrombus formation; however, physiologic levels (VWF:Ag < 1.5 U/mL) of transgenic wild-type mVWF were able to produce occlusive thrombi in these mice.<sup>29</sup>

Contrary to our initial hypothesis that circulating 2B VWF might act as a thrombogenic stimulus, the mice expressing the 2B VWD variants showed a marked failure of platelet accumulation and little or no thrombus formation after vascular damage. Most notably, less platelet adhesion was seen with the 2B VWD variants than was seen with VWF<sup>-/-</sup> mice. The cause for this enhanced deficiency in platelet adhesion, and thus, also the bleeding tendency in type 2B patients, is probably multifactorial and includes the following: (1) the thrombocytopenic phenotype seen with the 2B VWD variants; (2) the circulating platelet aggregates; (3) the absence of HMW VWF multimers; and (4) the absence of platelet and subendothelial VWF in this animal model. In addition, the GPIIb/IIIa receptors of the circulating platelets may be occupied by soluble VWF, preventing the initial adhesion of these platelets at sites of damage, thus preventing the activation and further accumulation of platelets at sites of vascular damage. Studies in which normal platelets were infused into mice expressing the V1316M mutation showed only a partial correction of the thrombogenic response, thus emphasizing the key role of the VWF plasma compartment in this condition. This observation, in the VWD 2B mouse model, suggests that the optimal therapeutic approach for this bleeding defect should probably first involve supplementation of the plasma VWF compartment (as is currently done with VWF concentrate infusions) and that platelet transfusions be used only in cases with severe thrombocytopenia or where bleeding is resistant to concentrate infusion.

In conclusion, these studies have recapitulated, in a mouse model of the disease, the variable, mutation-specific phenotypes seen in 2B VWD. This phenotypic variability was documented with mutant VWF present only in the plasma compartment. Of particular note, in an arteriolar thrombosis model, thrombus development and platelet adhesion were markedly diminished with the 2B mutant proteins, with platelet adhesion that was significantly reduced to that seen in VWF<sup>-/-</sup> mice. This latter finding suggests that the defect in platelet-dependent hemostasis in 2B VWD is highly significant.

## Acknowledgments

The authors thank Peter Lenting for provision of the mouse *Vwf* cDNA, Friedrich Scheiflinger for the mouse ADAMTS13 expression vector, Luigi Naldini for the synthetic ET promoter, and Jalna Meens (Queen's Cancer Research Institute) for help with the intravital microscopy studies.

This work was supported by funds from the Canadian Institutes of Health Research (operating grant MOP-97849). M.G. is the recipient of a Queen's University Graduate Scholarship and the Dr Robert J. Wilson Graduate Fellowship. D.L. holds a Canada Research Chair in Molecular Hemostasis.

## Authorship

Contribution: M.G. designed, performed, analyzed, and interpreted research, performed statistical analysis, and wrote the manuscript; C.M.P. performed and analyzed research; C.H., J.M., K.L., and K.S. performed research; and D.L. designed research, interpreted data, and wrote the manuscript.

Conflict-of-interest disclosure: The authors declare no competing financial interests.

Correspondence: David Lillicrap, Department of Pathology and Molecular Medicine, Richardson Laboratory, Queen's University, Kingston, ON, K7L 3N6 Canada; e-mail: lillicrap@cliff.path.queensu.ca.

## References

- Randi AM, Rabinowitz I, Mancuso DJ, Mannucci PM, Sadler JE. Molecular basis of von Willebrand disease type IIB: candidate mutations cluster in one disulfide loop between proposed platelet glycoprotein Ib binding sequences. *J Clin Invest*. 1991;87(4):1220-1226.
- Cooney KA, Ginsburg D. Comparative analysis of type 2B von Willebrand disease mutations: implications for the mechanism of von Willebrand factor binding to platelets. *Blood*. 1996;87(6):2322-2328.
- Ruggeri ZM. Type IIB von Willebrand disease: a paradox explains how von Willebrand factor works. *J Thromb Haemost*. 2004;2(1):2-6.
- Lillicrap D. Genotype/phenotype association in von Willebrand disease: is the glass half full or empty? *J Thromb Haemost*. 2009;7(suppl 1):65-70.
- Rayes J, Hommais A, Legendre P, et al. Effect of von Willebrand disease type 2B and type 2M mutations on the susceptibility of von Willebrand factor to ADAMTS-13. *J Thromb Haemost*. 2007;5(2):321-328.
- University of Sheffield. ISTH SSC VWF database. www.vwf.group.shef.ac.uk. Accessed October 24, 2009.
- Federici AB, Mannucci PM, Castaman G, et al. Clinical and molecular predictors of thrombocytopenia and risk of bleeding in patients with von Willebrand disease type 2B: a cohort study of 67 patients. *Blood*. 2009;113(3):526-534.
- Denis C, Methia N, Frenette PS, et al. A mouse model of severe von Willebrand disease: defects in hemostasis and thrombosis. *Proc Natl Acad Sci U S A*. 1998;95(16):9524-9529.
- Marx I, Lenting PJ, Adler T, Pendu R, Christophe OD, Denis CV. Correction of bleeding symptoms in von Willebrand factor deficient mice by liver-expressed von Willebrand factor mutants. *Arterioscler Thromb Vasc Biol*. 2008;28(3):419-424.
- Lenting PJ, de Groot PG, De Meyer SF, et al. Correction of the bleeding time in von Willebrand factor (VWF)-deficient mice using murine VWF. *Blood*. 2007;109(5):2267-2268.
- Shi CX, Graham FL, Hitt MM. A convenient plasmid system for construction of helper-dependent adenoviral vectors and its application for analysis of the breast-cancer-specific mammaprotein promoter. *J Gene Med*. 2006;8(4):442-451.
- Amendola M, Veneri MA, Biffi A, Vigna E, Naldini L. Coordinate dual-gene transgenesis by lentiviral vectors carrying synthetic bidirectional promoters. *Nat Biotechnol*. 2005;23(1):108-116.
- Pruss CM, Notley CR, Hegadorn CA, O'Brien LA, Lillicrap D. ADAMTS13 cleavage efficiency is altered by mutagenic and, to a lesser extent, polymorphic sequence changes in the A1 and A2 domains of von Willebrand factor. *Br J Haematol*. 2008;143(4):552-558.
- Stakiw J, Bowman M, Hegadorn C, et al. The effect of exercise on von Willebrand factor and ADAMTS-13 in individuals with type 1 and type 2B von Willebrand disease. *J Thromb Haemost*. 2008;6(1):90-96.
- Bruno K, Volkel D, Plaimauer B, et al. Cloning, expression and functional characterization of the full-length murine ADAMTS13. *J Thromb Haemost*. 2005;3(5):1064-1073.
- Gavins FN, Chatterjee BE. Intravital microscopy for the study of mouse microcirculation in anti-inflammatory drug research: focus on the mesentery and cremaster preparations. *J Pharmacol Toxicol Methods*. 2004;49(1):1-14.
- Dubois C, Panicot-Dubois L, Merrill-Skoloff G, Furie B, Furie BC. Glycoprotein VI-dependent and -independent pathways of thrombus formation in vivo. *Blood*. 2006;107(10):3902-3906.
- Ware J, Russell SR, Marchese P, Ruggeri ZM.

- Expression of human platelet glycoprotein Ib alpha in transgenic mice. *J Biol Chem.* 1993; 268(11):8376-8382.
19. De Luca M, Facey DA, Favalaro EJ, et al. Structure and function of the von Willebrand factor A1 domain: analysis with monoclonal antibodies reveals distinct binding sites involved in recognition of the platelet membrane glycoprotein Ib-IX-V complex and ristocetin-dependent activation. *Blood.* 2000;95(1):164-172.
  20. Fukuda K, Doggett T, Laurenzi IJ, Liddington RC, Diacovo TG. The snake venom protein botrocetin acts as a biological brace to promote dysfunctional platelet aggregation. *Nat Struct Mol Biol.* 2005;12(2):152-159.
  21. Szanto T, Schlamadinger A, Salles I, et al. Type 2B von Willebrand disease in seven individuals from three different families: phenotypic and genotypic characterization. *Thromb Haemost.* 2007; 98(1):251-254.
  22. Suda T, Liu D. Hydrodynamic gene delivery: its principles and applications. *Mol Ther.* 2007; 15(12):2063-2069.
  23. Nurden P, Chretien F, Poujol C, Winckler J, Borel-Derlon A, Nurden A. Platelet ultrastructural abnormalities in three patients with type 2B von Willebrand disease. *Br J Haematol.* 2000;110(3):704-714.
  24. Nurden P, Gobbi G, Nurden A, et al. Abnormal VWF modifies megakaryocytopoiesis: studies of platelets and megakaryocyte cultures from von Willebrand disease type 2B patients. *Blood.* 2010;105(13):2649-2656.
  25. Schmitt A, Guichard J, Masse JM, Debili N, Cramer EM. Of mice and men: comparison of the ultrastructure of megakaryocytes and platelets. *Exp Hematol.* 2001;29(11):1295-1302.
  26. Lacombe M, d'Angelo G. Etudes sur une thrombopathie familiale. *Nouv Rev Fr Hematol.* 1963;3: 611-614.
  27. Jackson SC, Sinclair GD, Cloutier S, Duan Z, Rand ML, Poon MC. The Montreal platelet syndrome kindred has type 2B von Willebrand disease with the VWF V1316M mutation. *Blood.* 2009;113(14):3348-3351.
  28. McKinnon TA, Chion AC, Millington AJ, Lane DA, Laffan MA. N-linked glycosylation of VWF modulates its interaction with ADAMTS13. *Blood.* 2008; 111(6):3042-3049.
  29. Golder M, Pruss CM, Hegadorn C, et al. Supraphysiological levels of plasma von Willebrand factor do not support primary hemostasis in von Willebrand factor knock-out mice. *J Thromb Haemost.* 2009;7(suppl 2): 1145.